

## SOME EXPERIMENTAL FORCE ANALYSIS FOR AUTOMATION OF EXCAVATION BY A BACKHOE

Ahmad Hemami ‡

Derek W. Seward §

Stephen Quayle §

‡ *Dept. of Mining and Metallurgical Engineering  
McGill University, Montreal, Que. H3A 2A7, Canada*

§ *Department of Engineering  
Lancaster University, Lancaster LA1 4YR, UK*

**Abstract** Automating the excavation function of an excavator is a complex control problem, because of the nature of the interaction between the cutting tool and the medium and the many parameters that are involved in the process. A fundamental question that is not yet resolved is the choice of parameters to be used in a feedback loop for the control of the process, and the control algorithm. Based on a previous proposition for the control algorithm to be used for this purpose, knowledge about the forces involved may be used for adjusting the motion of the bucket. In this paper, some results of experimental measurements of the excavation forces are presented. These forces cannot be measured directly on the bucket, but the kinematic and dynamic relations can serve for this purpose. The paper talks about the development of these relations, and then the results are presented and discussed.

**Keywords:** Automation, excavation, force measurement, kinematics, backhoe

### INTRODUCTION

Automation of excavation necessarily implies that an excavator carries out its function without being operated by a person. This function consists of one or more of cutting, digging, scooping and penetration into the medium to be excavated. Excavating machines are of different form, depending on the environment and/or the application. For example a backhoe is most suitable for excavating below ground, whereas a power shovel is designed to load its bucket from a higher level. With all excavating machines, the bucket or the excavating tool must interfere with the material to be excavated and, necessarily, must overcome the inherent resistance that it experiences from the medium. In other words, the tool must overcome the resistance from the environment it is dealing with. This resisting force, however, is a function of a large number of parameters dependent upon the medium, the tool and the environment. It also depends on the motion of the excavator's tool. In this sense, the value and the direction of the resistive force has a significant variation during the course of an excavation task, since it has a stochastic nature and, as yet, has not been mathematically modeled.

Considering the fact that the normally curvilinear motion of the bucket is provided by a set of actuators, it is essential that the required force by each actuator be furnished at each instant. This implies that each actuator must provide sufficient power in order to maintain the motion of the bucket. In practice, this is possible only if an enormous amount of power is available at each actuator, which is generally uneconomic. In the case of a human operator, a skilled person continuously adjusts the tool motion, by using his intelligence and experience, so that the final goal of excavation is accomplished. In fact, he adjusts the

motion when he feels that the tool motion is not what was intended. Otherwise, not only the task is not carried out properly, but the machine elements may get damaged, too.

Various approaches have been suggested on the matter and numerous work has been reported. Some of the reported works are listed in the References of the present paper. The main issue in automated excavation is successfully filling the bucket. There exist two extreme cases, both of which are unsatisfactory. Either the bucket gets stuck in a situation where an increase in force is useless, or the bucket continues its motion without being loaded. In the first case any more effort to move the bucket has no effect other than damaging the system (slipping and eroding the tires in a front-end loader, for instance). The second case, obviously, is not desirable, either.

In previous work [3] it was suggested that, by finding the envelope of the maximum and minimum excavation force during a specific excavation task, one can avoid the two extreme cases. By "specific" it is meant that a given bucket (fixed physical dimensions) has a well defined motion (fixed trajectory) to excavate from a medium that by a common judgement is fixed (water content, density, size and other characteristics have no dramatic variations), and the environmental conditions (temperature and gravity) do not introduce phase changes (freezing, for instance). In this way, by measurement of the excavation force as a feedback parameter, the bucket motion can be readjusted anytime the experienced force is outside of its expected limits.

In this paper, some results of experimental measurement of excavation forces are presented. For this purpose, first, the kinematic and force relationships for a typical backhoe excavator are derived.

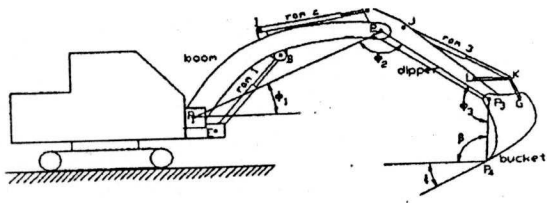


Figure 1

## KINEMATIC MODELING

Figure 1 shows the schematic of the system under study and certain variables and definitions. System kinematic relationships are necessary for the transformation of the desired cutting path and velocities in individual joint movements. The Denavit-Hartenberg coordinate system assignment will be employed. For reasons of simplicity we will ignore the slewing of the cab about the vehicle tracks. The other joint motions take place, more or less, in plane. Thus a planar analysis is sufficient, and the cutting edge will be represented by a point. The choice of coordinate systems is similar to that of the work of Vähä et al [12], except for the deletion of the first coordinate system  $X_0Y_0Z_0$  (for the inclusion of slew motion) which in our case is the same as the shown  $X_1Y_1Z_1$ . Thus the transformation between the reference frame and the first frame is the identity matrix.

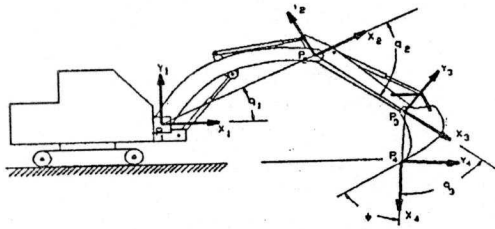


Figure 2

Figure 2 shows the various coordinate systems. The associated transformation matrices are as follows:

$$A_1 = \begin{bmatrix} C_1 & -S_1 & 0 & a_1C_1 \\ S_1 & C_1 & 0 & a_1S_1 \\ 0 & 0 & 1 & 0 \\ 0 & 0 & 0 & 1 \end{bmatrix} \quad (1)$$

$$A_2 = \begin{bmatrix} C_2 & -S_2 & 0 & a_2C_2 \\ S_2 & C_2 & 0 & a_2S_2 \\ 0 & 0 & 1 & 0 \\ 0 & 0 & 0 & 1 \end{bmatrix} \quad (2)$$

$$A_3 = \begin{bmatrix} C_3 & -S_3 & 0 & a_3C_3 \\ S_3 & C_3 & 0 & a_3S_3 \\ 0 & 0 & 1 & 0 \\ 0 & 0 & 0 & 1 \end{bmatrix} \quad (3)$$

where S and C stand for  $\sin(\cdot)$  and  $\cos(\cdot)$ , respectively, and the subscripts 1-3 denote the assigned number of a joint and its associated coordinate system. The parameter  $a$ 's are the joint lengths based on the D-H parameter definition; the twist angles are all zero for the simple planar robot

arm of the excavator. The joint variables are represented by  $q$  and the other angles, required for geometric or mathematical relationships, are as shown in the figures 3 and 4.

For consistency with previous work, some additional variables are defined such as the manufacture's maximum and minimum values of each joint angle. The lengths  $l_1$  to  $l_{25}$  are geometric dimensions. From these, only those pertinent to the studies and used in this paper are shown. Based on these definitions, the corresponding values for the joint lengths are as follow:

$$a_1 = l_1, \quad a_2 = l_2, \quad \text{and} \quad a_3 = l_3 \quad (4)$$

The coordinates of the cutting edge of the bucket with respect to the reference coordinate system are given by

$$x = a_1C_1 + a_2C_{12} + a_3C_{123} \quad (5)$$

and

$$y = a_1S_1 + a_2S_{12} + a_3S_{123} \quad (6)$$

and the orientation of the bucket,

$$\beta = q_1 + q_2 + q_3 \quad (7)$$

where  $C_1 = \cos(q_1)$ ,  $C_{12} = \cos(q_1 + q_2)$  and  $C_{123} = \cos(q_1 + q_2 + q_3)$ , and likewise for  $S_1$ ,  $S_{12}$  and  $S_{123}$ .

However, if the angle of the bucket teeth,  $\phi$  is required, the constant value of the angle  $\psi$  must be added to it. This orientation is with respect to the untilted body of the backhoe. If the machine has an angle  $\mu$  with the horizontal plane and the angle of the bucket with a horizontal plane is desired, then the angle  $\mu$  must be added to the said values. The positive direction of all the angles are counterclockwise for the configuration of the excavator shown in the figures.

The Jacobian matrix is used to relate the velocities and the forces at a given point of interest on a robot arm with respect to a desired coordinate frame. The Jacobian matrix for the system under study, defining the motion of the tool point (the cutting edge of the bucket), with respect to frame 1 is as follows:

$$J = J'_1 = \begin{bmatrix} -a_1 \sin(q_1 + q_2 + q_3) - a_2 \sin(q_1 + q_2) - a_3 \sin q_1 \\ a_1 \cos(q_1 + q_2 + q_3) + a_2 \cos(q_1 + q_2) + a_3 \cos q_1 \\ -1 \\ -a_2 \sin(q_1 + q_2 + q_3) - a_2 \sin(q_1 + q_2) - a_3 \sin(q_1 + q_2 + q_3) \\ a_2 \cos(q_1 + q_2 + q_3) + a_2 \cos(q_1 + q_2) \quad a_3 \cos(q_1 + q_2 + q_3) \\ -1 \quad -1 \end{bmatrix} \quad (8)$$

## INVERSE KINEMATICS

Inverse kinematics implies finding the values for the joint angles,  $q_1$ ,  $q_2$  and  $q_3$  when the position and orientation of the cutting edge is known with respect to the reference frame  $X_0Y_0Z_0$ . It follows from equations (5) to (7) that when  $\beta$  is known, then  $q_{123}$  is known and having  $x$  and  $y$  leads to:

$$a_1 \cos q_1 + a_2 \cos(q_1 + q_2) = x \quad (9)$$

and

$$a_1 \sin q_1 + a_2 \sin(q_1 + q_2) = y \quad (10)$$

These are two equations in two unknowns; their solution can be easily found, as shown in Appendix B. Once solved, then the values of  $q_1$ ,  $q_2$  and  $q_3$  are readily determined.

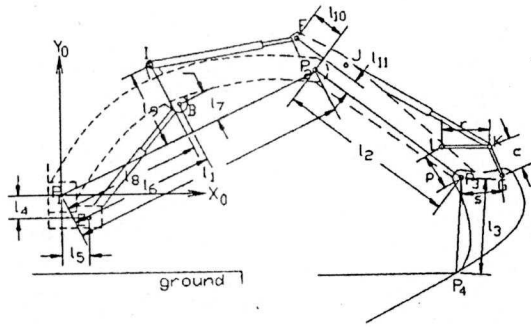


Figure 3

The other necessary calculations are the relationships between the ram lengths (actuator variables) and the position and orientation of the cutting teeth of the bucket, and the ram forces and the corresponding cutting/loading forces the bucket must exert to its environment.

The relationship between the length of the first actuator and its corresponding joint variable  $q_1$  is

$$ram\ 1 = \sqrt{l_5^2 + l_4^2 + l_3^2 - 2l_5[l_4 \cos(q_1 + \eta) + l_3 \sin(q_1 + \eta)]} \quad (11)$$

where  $\eta$  is the angle  $\angle BP_1 P_2$ , which is constant, and

$$l_b = \sqrt{l_6^2 + l_7^2}$$

Equation (11) can be used, also, to find the magnitude of  $q_1$  in terms of the actuator length. The corresponding equation is in the general form of

$$m_0 \sin(q_1 + \eta) + n_0 \cos(q_1 + \eta) = h_0 \quad (12)$$

where

$$m_0 = \frac{l_4}{2\sqrt{l_6^2 + l_7^2}}; \quad n_0 = \frac{l_3}{2\sqrt{l_6^2 + l_7^2}} \quad \text{and} \quad h_0 = l_4^2 + l_3^2 + l_6^2 + l_7^2 - (ram\ 1)^2$$

This equation has generally two answers, but only one of them is acceptable for the system under study. These answers are

$$q_1 = \tan^{-1}(h_0, \pm \sqrt{m_0^2 + n_0^2 - h_0^2}) - \tan^{-1}(n_0, m_0) - \eta \quad (13)$$

In equation (13),  $\tan^{-1}$  stands for atan2 function.

In a similar manner, the length of the actuator 2 in terms of angle  $q_2$  is

$$ram\ 2 = \sqrt{(l_1 - l_8)^2 + l_5^2 + l_7^2 - 2l_f[(l_1 - l_8)\cos(\gamma - q_2) + l_5 \sin(\gamma - q_2)]}$$

where  $\gamma$  is the constant angle  $\angle FP_2 P_3$  and  $l_f$  is the distance between points  $P_2$  and  $F$ , and in terms of the dimensions shown in figure 3 is

$$l_f = \sqrt{l_{10}^2 + l_{11}^2} \quad (15)$$

The magnitude of angle  $q_2$  in terms of the ram length is found from

$$q_2 = \gamma - \tan^{-1}(d, \pm \sqrt{l_5^2 + (l_1 - l_8)^2 - d^2}) - \tan^{-1}[(l_1 - l_8)/l_5] \quad (16)$$

where

$$d = \frac{(l_1 - l_8)^2 + l_5^2 + l_f^2 - (ram\ 2)^2}{2l_f}$$

The relationships for the third joint are more complicated, because of the four-bar linkage. Changing the length of ram 3 leads to changes in the angles of the linkage, which govern the bucket motion. The four-bar linkage is shown in figure 4. The lengths of the sides are represented by  $c$ ,  $p$ ,  $r$  and  $s$ . In a classical linkage the input angle is  $\lambda$  and the output angle is  $\alpha$ . In our case, however, we are interested in the relationship between the actuator length and its joint angle  $q_3$ . The length of ram 3 can be defined as

$$ram\ 3 = \sqrt{l_{24}^2 - 2l_{24}[(l_{22} - l_{27})\sin \lambda_3 - (l_{21} - l_{28})\cos \lambda_3] + (l_{22} - l_{27})^2 + (l_{21} - l_{28})^2} \quad (17)$$

where all the elements are as shown in figure 4. Here, instead of  $\lambda$  another angle  $\lambda_3$  (see figure 4) is employed. When necessary, the following relationships can be used.

$$\lambda_1 = \tan^{-1} \frac{l_{21}}{l_{22}} \quad \text{and} \quad \lambda_2 = \pi - \lambda \quad (18)$$

$$\text{and} \quad \lambda_3 = \pi - \lambda_2 - \lambda \quad (19)$$

$$\text{so that} \quad \sin \lambda_3 = \cos(\lambda_1 - \lambda) \quad \text{and} \quad \cos \lambda_3 = \sin(\lambda - \lambda_1) \quad (20)$$

The following relationship holds between  $\lambda_3$  and  $\alpha$ :

$$(l_{22} - r \sin \lambda_3)^2 + (l_{21} + r \cos \lambda_3)^2 + 2s \sin \alpha (l_{22} - r \sin \lambda_3) - 2s \cos \alpha (l_{21} + r \cos \lambda_3) = c^2 - s^2 \quad (21)$$

From this equation we can derive  $\alpha$  in terms of  $\lambda_3$  or vice versa. In order to find  $\alpha$  the resulting equation is in the form of

$$m_1 \sin \alpha + n_1 \cos \alpha = h_1 \quad (22)$$

$$\text{where} \quad m_1 = -(l_{21} + r \cos \lambda_3) \quad n_1 = (l_{22} - r \sin \lambda_3)$$

and

$$h_1 = \frac{1}{2s}(c^2 - s^2 - r^2 - p^2) - \frac{r}{s}(l_{21} \cos \lambda_3 - l_{22} \sin \lambda_3)$$

The solution to this equation is given in appendix A. The same solution applies for the case of determining  $\lambda_3$  in terms of  $\alpha$ , whose equation is

$$m_2 \sin \lambda_3 + n_2 \cos \lambda_3 = h_2 \quad (23)$$

where





force components experienced during the five experiments.

In the figures shown, the horizontal axis shows the sampling number of the measurement taken, and is proportional to time. The values on the vertical axis in figures 5, 6 and 7 denote the voltage of the signal from the pressure transducer. A reading of .5 volt represents zero pressure and 4.5 volt corresponds to a pressure of 350 bars. The force values in figures 8 to 10 are in Newton.

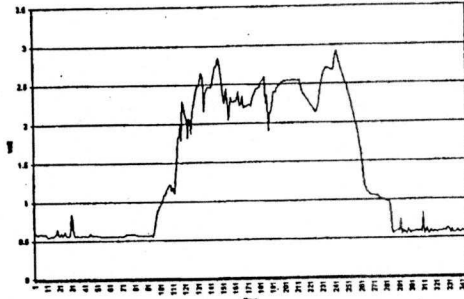


Figure 5- A typical reading of boom ram pressure

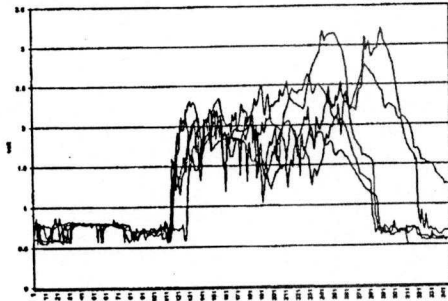


Figure 6- Pressure variation in the boom ram - all runs

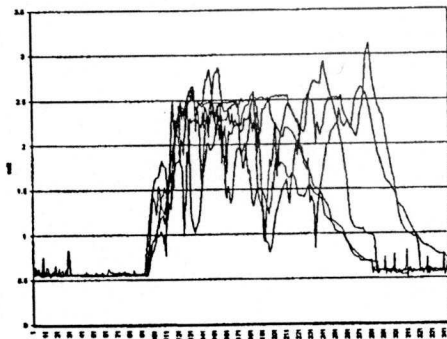


Figure 7- Pressure variation in the dipper ram- all runs

### DISCUSSION

The desired outcome of the study is that, for every point on a given trajectory of the cutting edge of the bucket there should be a maximum and minimum value of excavation force, for a given bucket and a specific medium. The results obtained fulfil this requirement to a certain degree, only. The problem lies in the fact that the speed of operation also has an effect on the results. As it can be seen from the figures 9 and 10, the starting points coincide whereas

the finishing times are not necessarily the same. However, as the number of trials is increased, this difference becomes less and less significant. Consequently, it can be said that the assumption of maximum and minimum values of the excavation force, is correct.

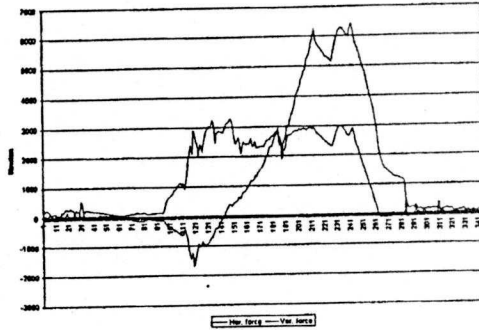


Figure 8- A typical sample of excavation force

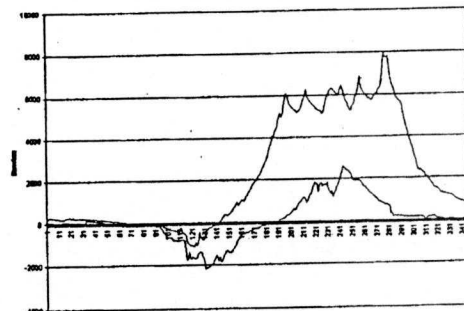


Figure 9 - Maximum and minimum of excavation force horizontal component

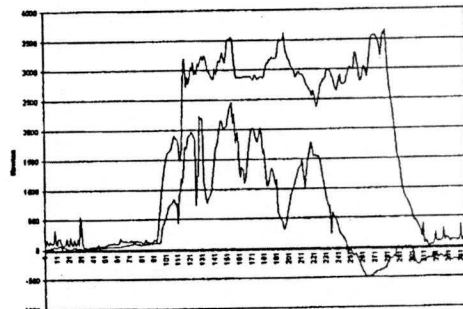


Figure 10 - Maximum and minimum of excavation force vertical component

### SUMMARY

This paper presents some analytical results for the kinematics and force relationships in a typical backhoe. These relationships are required for the feedback purposes at both higher and lower level control of the motion of bucket for automating the excavation process of such a machine. Also, experimental results of the measurement of the excavation force are presented that confirm an assumption of previous work regarding the variation of such a force during an excavation task.

## REFERENCES

- [1] Bernold L.E., "Motion and Path Control for Robotic Excavation", *J. Aerospace Engineering*, Vol. 6, pp 1-18, 1993.
- [2] Bullock, D. M., Apte, S. M. and Oppenheim, I. J., "Force and Geometry Constraints in Robot Excavation", *Proc. Space 90 Conf. Part 2, Albuquerque*, pp 960-969, 1990.
- [3] Hemami, A., "Study of Bucket Trajectory in Automatic Scooping with Load-Haul-Dump Loaders", *Trans. Inst. Mining and Metall., Sect. A, Vol 102, Jan.*, pp A37-A42, 1993.
- [4] Hemami, A., "Study of Forces in the Scooping Operation of a Mechanical Loader", *Trnas. CSME (Canadian Soc. of Mechanical Engineers)*, Vol. 18, No. 3, pp 191-205, 1994
- [5] Hemami, A., A Fundamental Analysis of Robotic Excavation, *J. of Aerospace Engineering*, Vol. 8, No. 4, , pp 783-790, 1995.
- [6] Koivo, A. J. "Planning for Automatic Excavator Operations", *Proc. the 9th Int. Symp. on Aut. and Robotics in Construction*, , Tokyo, pp 869-878, 1992
- [7] Novak, A.J. and Larson, C., "A Computer Simulation of Backhoe Type Excavators", *SAE special publications No. 884*, Sept, pp 41-48, 1991.
- [8] Seward, D, D Bradley and R Bracewell "The Development of research models for automatic excavation.", *5th Int. Symp. on Robotics in Construction*, Tokyo, Vol. 2, pp 703 - 708 (June 1988).
- [9] Seward, D., Bradley, D., Mann, J. and Goodwin, M., "Controlling an Intelligent Excavator for Automated Digging in Difficult Ground", *Proc. the 9th Int. Symp. on Aut. and Robotics in Construction*, Tokyo, pp 743-750, June 1992.
- [10] Shi, X, F-Y Wang and, P.J. A Lever, "Task and Behaviour Formulation for Robotic Rock Excavation", *Proc. 10th IEEE Int. Symp on Intelligent Control*, pp 247-253, 1995
- [11] Shi, X, Lever, P.J. A and F-Y Wang, "Experimental Robotic Excavation with Fuzzy Logic and Neural Networks", *Proc. IEEE Int. Conf. Robotics and Automation, Vol.1*, pp957-962, 1996
- [12] Sing, S, "An Operation Space Approach to Robotic Excavation", *Proc. IEEE Int. Symp. Int. Control.*, NY, 481-486, 1991
- [13] Vaehae, P. K., Skibniewski, M. J. and Koivo, A. J., "Kinematics and Trajectory Planning for Robotic Excavation", *Proc. Construction Congress 91*, Cambridge, MA, , pp 787-793, 1991.
- [14] Vaehae, P. K., Koivo, A. J. and Skibniewski, M. J., "Excavation Dynamics and Effect of Soil on Digging", *Proc. the 8th Int. Symp. on Automation and Robotics in Construction*, , Stuttgart, pp 297-306, June 1991.

## APPENDIX A

The general solutions to a trigonometric equation of the form

$$m \sin x + n \cos x = h$$

is obtained by, first, writing the equation in the equivalent form

$$\frac{m \sin x}{\sqrt{m^2 + n^2}} + \frac{n \cos x}{\sqrt{m^2 + n^2}} = \frac{h}{\sqrt{m^2 + n^2}}$$

Setting

$$\frac{m}{\sqrt{m^2 + n^2}} = \cos y \quad \text{and} \quad \frac{n}{\sqrt{m^2 + n^2}} = \sin y$$

leads to

$$\sin(x + y) = \frac{h}{\sqrt{m^2 + n^2}} \quad \text{and} \quad \cos(x + y) = \frac{\pm \sqrt{m^2 + n^2 - h^2}}{\sqrt{m^2 + n^2}}$$

and the value of the unknown  $x$  is, then

$$x = \tan^{-1}\left(\frac{h}{\pm \sqrt{m^2 + n^2 - h^2}}\right) - y$$

## APPENDIX B

In the set of equations (9) and (10)  $x$  and  $y$  are known and  $q_1$  and  $q_2$  are the two unknowns. can be solved as follows. By rearranging the equations we have

$$x - a_1 \cos q_1 = a_2 \cos(q_1 + q_2)$$

$$y - a_1 \sin q_1 = a_2 \sin(q_1 + q_2)$$

Squaring each side and adding together leads to

$$x^2 + y^2 - 2a_1[y \sin q_1 + x \cos q_1] + a_1^2 = a_2^2$$

or

$$y \sin q_1 + x \cos q_1 = \frac{x^2 + y^2 + a_1^2 - a_2^2}{2a_1}$$

This equation is in the same form as solved in Appendix A. When solved then the magnitude of  $q_2$  can, further, be readily found.